The Canadian Mineralogist
Vol. 41, pp. 457-472 (2003)

SULFIDE FORMATION RELATED TO CHANGES IN THE HYDROTHERMAL SYSTEM ON LOIHI SEAMOUNT, HAWAI'I, FOLLOWING THE SEISMIC EVENT IN 1996

ALICÉ S. DAVIS[§] AND DAVID A. CLAGUE

Research and Development Division, Monterey Bay Aquarium Research Institute, 7700 Sandholdt Road, Moss Landing, California 95039-9644, U.S.A.

ROBERT A. ZIERENBERG

Department of Geology, University of California, Davis, One Shields Avenue, Davis, California 95616-8605, U.S.A.

C. GEOFFREY WHEAT

Institute of Marine Sciences, University of Fairbanks, P.O. Box 475, Moss Landing, California 95039, and Monterey Bay Aquarium Research Institute, 7700 Sandholdt Road, Moss Landing, California 95039-9644, U.S.A.

BRIAN L. COUSENS

Department of Earth Sciences, Carleton University, 1125 Colonel By Drive, Ottawa, Ontario K1S 5B6, Canada

ABSTRACT

Hydrothermal sulfide and sulfate minerals were discovered in sediment samples collected on the Rapid Response Cruise to Loihi Seamount, following a large swarm (>4000) of earthquakes in the summer of 1996. *PISCES V* submersible dives, conducted two months after the seismic event, discovered that part of the summit had collapsed to form a new pit crater. The sudden collapse of the summit crater resulted in a cataclysmic discharge of hydrothermal fluid, ejecting magmatic gases and sulfide crystals. The presence of wurtzite, pyrrhotite, and chalcopyrite indicate high-temperature fluids (>250°C), the first such occurrence documented for an ocean-island volcano. The composition of the sulfide minerals is similar to that of sulfides from black smokers at mid-ocean ridges. Samples from barite-rich mounds, built after the initial cataclysmic discharge of the hydrothermal plume, resemble white smoker deposits from mid-ocean ridges. The $\delta^{34}S$ of the sulfide is lower than that of minerals from massive sulfide deposits formed on oceanic basalt, suggesting that the Loihi basalt has lost sulfur as magmatic SO_2. Dissolution and oxidation of the ejected high-temperature sulfides, observed over the two years following the event, suggest that these minerals are not easily preserved. Similar crystals forming at deeper levels in the hydrothermal system probably are ejected repeatedly when volcanic and tectonic activity disrupts the hydrothermal system.

Keywords: Loihi Seamount, hydrothermal, massive sulfide, chemical composition, mineralogy, mineral chemistry, sulfur isotopes, Hawai'i.

SOMMAIRE

Nous avons trouvé des sulfures et des sulfates hydrothermaux dans les échantillons de sédiment prélevés lors d'une mission d'urgence au guyot Loïhi à la suite d'une grande activité sismique (>4000 événements) à l'été de 1996. A la suite de plongées du véhicule submersible *PISCES V* deux mois après le paroxysme, nous avons découvert qu'une partie du sommet s'était effondrée pour former un nouveau cratère. L'effondrement soudain du cratère sommital a causé une décharge cataclysmique de fluide hydrothermal, avec un complément de gaz magmatiques et de cristaux de sulfures. Nous signalons la présence de wurtzite, pyrrhotite, et chalcopyrite, indications de la présence d'un fluide à température élevée (>250°C), le premier exemple à être signalé près d'une île océanique. La composition des sulfures ressemble à celle des sulfures associées aux panaches noirs des évents près des rides océaniques. Les échantillons d'accumulations de débris riches en barite, construits après la décharge initiale du panache hydrothermal, ressemblent aux produits retrouvés dans les panaches blancs près des rides océaniques. Le rapport $\delta^{34}S$ des sulfures est inférieur à celui des minéraux des gisements de sulfures massifs associés aux basaltes océaniques, ce qui laisse

§ *E-mail address*: davisa@mbari.org

supposer que le basalte à Loïhi a perdu du soufre sous forme de SO_2 magmatique. La dissolution et l'oxydation des sulfures éjectés à température élevée, observées au cours des deux années suivant le cataclysme, nous poussent à croire que ces minéraux sont éphémères. Des cristaux semblables à des profondeurs plus grandes dans le système hydrothermal sont probablement projetés de façon semblable et répétée lors de disruptions du système hydrothermal par l'activité volcanique et tectonique.

(Traduit par la Rédaction)

Mots-clés: guyot de Loïhi, hydrothermal, sulfures massifs, composition chimique, minéralogie, composition des minéraux, isotopes de soufre, Hawai'i.

Introduction

Hydrothermal activity leading to the deposition of massive sulfides and sulfate at mid-ocean ridges has been studied extensively (*e.g.,* Hannington *et al.* 1995, and references therein). Long-lived hydrothermal systems at some spreading centers have created large mounds and dramatic chimney structures that can reach 45 m in height (Robigou *et al.* 1993). Formation of hydrothermal deposits is not confined to spreading centers, but also occurs in back-arc and fore-arc basins (*e.g.,* Both *et al.* 1986, Iizasa *et al.* 1992) and in some intracontinental rifts like the Red Sea (*e.g.,* Scholten *et al.* 2000). In fact, the first discovery of such metalliferous deposits was made in the sediment-covered basin of the Red Sea (Degens & Ross 1969).

Ubiquitous hydrothermal alteration of submarine erupted lava from ocean-island volcanoes testifies to the existence of such systems on these volcanoes. However, no massive hydrothermal deposits comparable to those at spreading centers have been described from an ocean island volcano.

Hydrothermal sulfide and sulfate minerals were discovered in sediment samples (Davis & Clague 1998) collected on the Rapid Response Cruise to Loihi Seamount, following a seismic event in the summer of 1996 (Loihi Science Team 1997). On follow-up cruises in the fall of 1997 and 1998, scientists observed that barite-rich mounds had formed at several active vent sites. In this study, we describe the hydrothermal minerals collected from the sediment and outcrops. On the basis of the samples recovered, we examine the evolution of the hydrothermal system on Loihi over the period of three years. We compare the composition of minerals and bulk samples to that of samples of hydrothermal origin from other tectonic settings.

Geological Setting and History of Hydrothermal Activity

Loihi Seamount is the youngest Hawaiian volcano. Located about 30 km southeast of the island of Hawai'i (Fig. 1A), it rises from a depth of about 4700 m to 980 m below sea level (Moore *et al.* 1982, Fornari *et al.* 1988). Prior to 1996, the summit area consisted of a platform with volcanic cones along the perimeter and two pit craters, 300 and 370 m deep (Fornari *et al.* 1988). Only low-temperature (<30°C) hydrothermal activity, primarily at the summit – south rift intersection, had been observed prior to 1996 (Malahoff *et al.* 1982, DeCarlo *et al.* 1983, Karl *et al.* 1988, Sakai *et al.* 1987, Sedwick *et al.* 1992, 1994). Diffuse venting was observed at two prominent vent fields, named Pele's and Kapo's vents, located at the base of pillow lava cones in the upper portion of the south rift. Extensive deposits of red-orange sediment, composed of iron-rich smectite and iron oxide, were found covering the talus surrounding the vents (DeCarlo *et al.* 1983, Karl *et al.* 1988). Malahoff *et al.* (1982) speculated that sulfide mineralization might be forming beneath the hydrothermal oxide deposits in the subsurface of Loihi.

A large swarm (> 4000) of earthquakes occurred on Loihi Seamount between July 16 and August 9, 1996 (Loihi Science Team 1997), which resulted in significant changes in the hydrothermal system. *PISCES V* submersible dives in August and October of 1996, following the seismic swarm, discovered a new pit crater 600 m in diameter and more than 300 m below the original surface, at the site of the former Pele's vents. Hydrothermal vents, named the Loihau vents, having measured temperatures of as much as 77°C, were discovered near the rim of the north wall of the new pit crater, which was named Pele's Pit (Fig. 1A). Significant thermal anomalies and ^{3}He enrichment of 150% were measured in the water column following the seismic swarm, indicating significant addition of heat and magmatic gases into the water column during the short-lived episode (Loihi Science Team 1997, Hilton *et al.* 1998). Sites of the 1996 dives and some additional sites were visited on five dives in 1997. The additional sites focused on active venting within the newly formed Pele's Pit, which was not investigated in 1996 because of poor visibility and safety concerns. Four additional dives were conducted in 1998, most of which centered on the warmer vents within Pele's Pit (Table 1, Fig. 1B). Fluid flow observed in 1997 was only a small fraction of that observed the previous year (Wheat *et al.* 2000), and the extent of fluid flow and of vent temperatures decreased further between repeat visits from 1997 to 1998. The most active venting occurred within the northeast corner of Pele's Pit at the base of a steep wall, where maximum temperatures of 200°C were recorded at some vents. Active bacterial mats were observed near vent edifices, and much of the entire area was covered with red- or orange-colored sediment. Near sites of active venting, barite-rich mounds up to 1 m in diameter

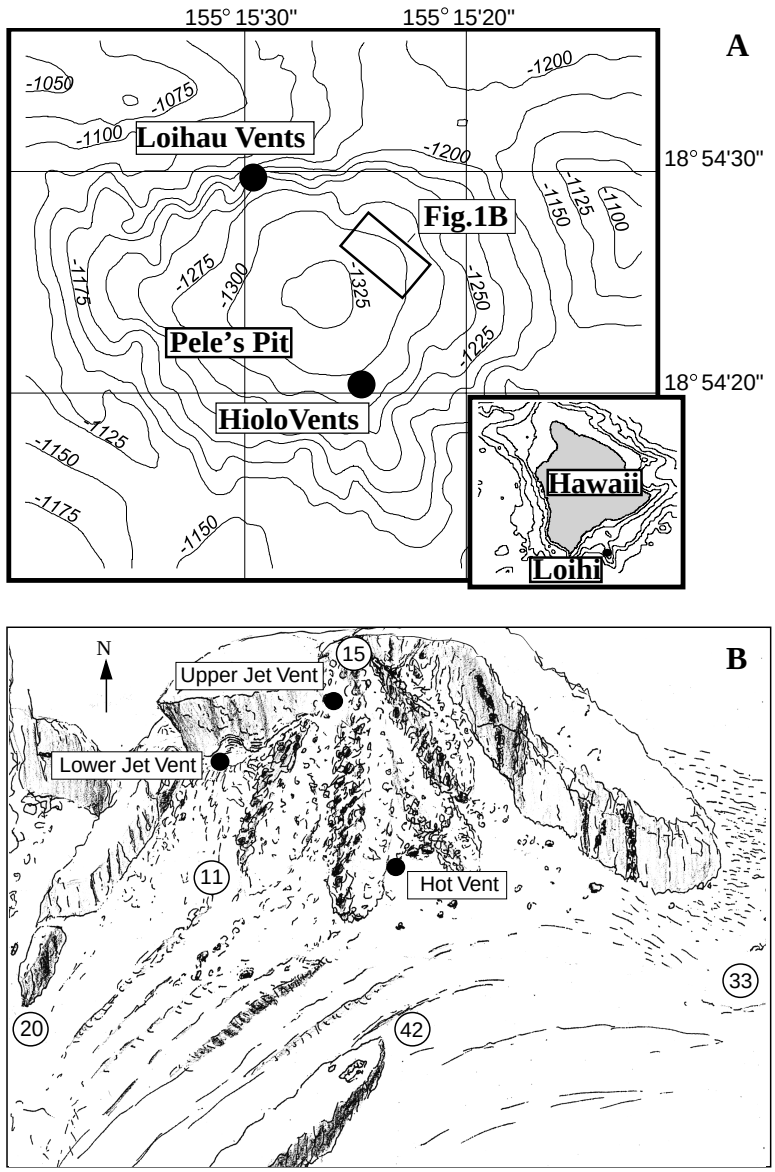

FIG. 1. A. Bathymetric map of the summit of Loihi Seamount, showing vent locations. Box indicates the area shown in the sketch (B), with vent and marker sites listed in Table 1. Inset shows location of Loihi relative to the island of Hawai'i.

and several tens of centimeters high were located (Fig. 2).

SAMPLING AND ANALYTICAL METHODS

Sulfide and sulfate particles were recovered in sediment scoops collected in talus on the north rim of Pele's pit near the Loihau Vents on *PISCES V* dives 310 and 316 in September 1996. Similar particles were collected in sediment scoops within Pele's Pit on *PISCES V* dives in 1997 and 1998. In addition, bulk samples from barite-rich mounds were collected with the manipulator arm on these later dives. Additional hydrothermal material encrusted the inside and outside of continuous water

samplers (OsmoSamplers) that were deployed in October 1996 and retrieved in September 1997 (Wheat *et al.* 2000).

Single crystals and clusters of crystals were hand-picked under a binocular microscope and mounted for either scanning electron microscopy (SEM) and mineral identification by X-ray energy-dispersion (EDS) analysis, complemented by X-ray diffraction (XRD). Polished thin sections were prepared of bulk samples of sulfate and of crystals in grain mounts for electron-microprobe analysis. Mineral compositions were determined with a JEOL JXA 8900 microprobe in the analytical laboratories of the U.S. Geological Survey in Menlo Park, California, using natural and synthetic mineral standards. Analytical precision is 1 to 2% for major elements and 5 to 7% for trace elements. Chemical analyses of bulk samples were performed by Activation Laboratories Ltd. (ACTLABS) in Ancaster, Ontario, Canada. Concentrations of the major elements, Zn and Cd were determined by Fusion ICP (inductively coupled plasma). Additional trace elements, including the rare earths, were determined by ICP–MS. Levels of sulfur and SO_4 were established by infrared (LECO) techniques. Details of analytical methods, accuracy and precision are available from actlaba@ibm.net. Sr isotopic analyses of selected crystals of barite were performed at Carleton University in Ottawa, using methods described by Cousens (1996). Proportions of sulfur isotopes in sulfide and sulfate crystals were determined on hand-picked crystals at the University of California at Davis, using a continuous-flow mass spectrometer in-

TABLE 1. SAMPLE LOCATION, WATER DEPTH AND MAXIMUM TEMPERATURE, LOIHI SEAMOUNT, HAWAI'I

Sample	Location	Water depth m	Max. T °C
P5-316 SC2	Loihau Vent	1173	77
P5-336 R2	New Vent	1303	190
P5-336 SC4	Hot Vent	1305	194
P5-336 SC7	New Vent	1303	190
P5-337 SC1	Hiolo Vent	1288	59
P5-340 R2	UpperJet Vent	1296	168
P5-340 SC2	Marker 42	1312	176
P5-341 R2	Marker 33	1302	193
P5-341 SC1	Marker 20	1310	107
P5-341 SC8	Hot Vent	1305	194
P5-341 SC9	Upper Jet Vent	1296	168
P5-398 SC1	Marker 11	1303	194
P5-398 SC2	Marker 15	1289	166
P5-398 SC4	Lower Jet Vents	1297	200
P5-398 M11	Marker 11	1303	194
P5-403 M15	Marker 15	1289	166

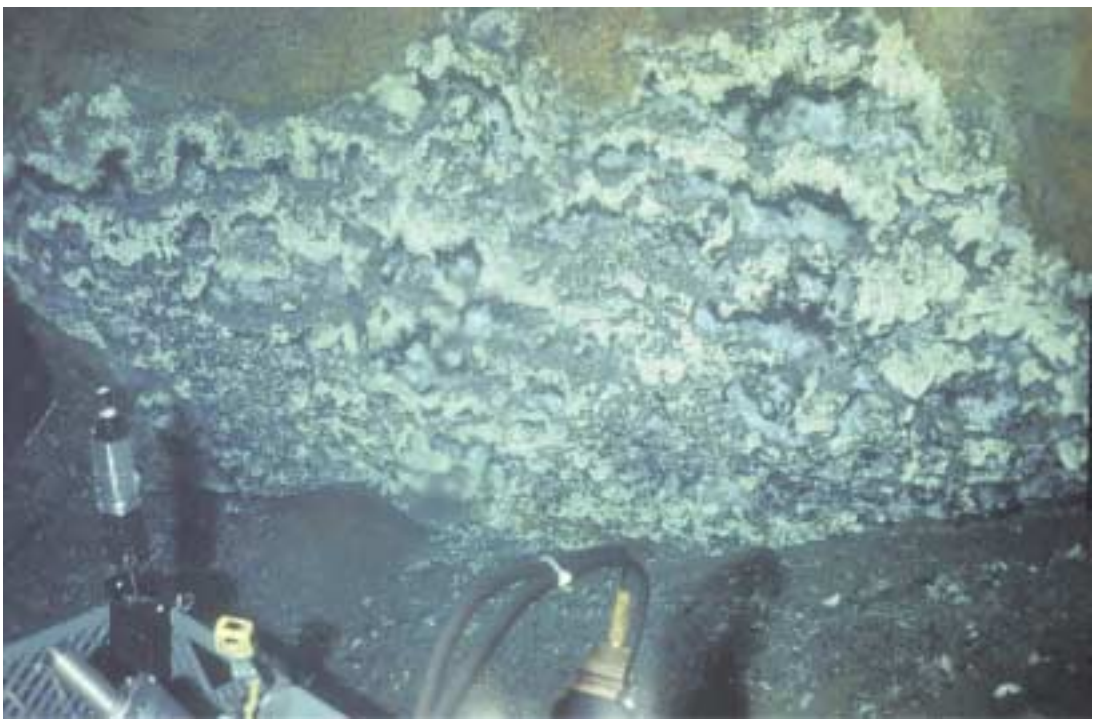

FIG. 2. Hydrothermal venting from barite-rich mounds observed on *PISCES V* dives in 1997. Field of view is approximately 1 m.

terfaced with an auto-analyzer for sample combustion and purification. The data are standardized against the NIST/IAEA reference materials S–1, S–2, and S–3, with accepted values of –0.3‰, 22.67‰, and –32.55‰, respectively (Ding *et al.* 2001).

Mineralogy and Petrography

The most distinctive features of the disseminated sulfide and sulfate particles collected in sediment scoops in 1996 are the large size, euhedral shape, and the virtually unoxidized surfaces of many of the sulfide crystals. Some large crystals of barite (to 0.3 cm) are euhedral and tabular (Fig. 3A), or doubly terminated pyramidal crystals (Fig. 3B), and may have inclusions of either Zn sulfide or pyrrhotite (Fig. 3A). Iron and zinc sulfide crystals of relatively large size (to ~2 mm) with euhedral shapes were also found in the sediment (Figs. 3C–F). Pyrite is the most abundant sulfide among the samples collected. Some of the pyrite forms hemispherical aggregates of euhedral, cubic crystallites on rock and glass fragments; others are irregularly shaped aggregates of striated cubes or pyritohedra, and some form botryoidal masses. The least abundant sulfide mineral in the 1996 collection is zinc sulfide, which occurs as black, shiny, hexagonal crystals with the morphology typical of wurtzite (Figs. 3D, E). Both wurtzite and sphalerite were identified by X-ray diffraction. Inclusions containing significant amounts of copper were discovered with the SEM in numerous samples of zinc sulfide. Pb- and Cd-rich inclusions also were found, mostly in zinc sulfide and rarely in pyrite. Pyrrhotite occurs as metallic, trigonal or pseudohexagonal crystals virtually devoid of oxidation (Fig. 3C) in the 1996 samples. Sulfide minerals from the 1997 collection are extensively covered with iron oxide, and many show an overgrowth of barite and pyrite crystals (Fig. 3F). Oxidation of sulfide minerals appears progressively more severe for samples collected from 1996 to 1998.

The bulk samples collected from the barite-rich mounds in 1997 and 1998 are predominantly breccias of sulfate with variable proportions of volcanic glass fragments (Figs. 4A–C). The glass-rich bulk samples look like hyaloclastite with a sulfate matrix. The fluidal-shaped and bubble-wall glass fragments (Fig. 5A) suggest formation in strombolian eruptions (Clague *et al.* 2000, 2003a). The glass spheres (Fig. 5B) suggest an origin in fire fountains (Vergniolle & Mangan 2000). The glass fragments show no evidence of hydrothermal alteration at their margins, although they are cemented by and encased in sulfide or sulfate minerals (Figs. 5A–C). Rare samples of siltstone, cemented by interstitial sulfate minerals, also were collected. The sulfate occurs in a network of capillaries and veinlets aligned along bedding planes (Fig. 4B). Samples collected from the hydrothermal mounds in 1998 consist of concentric layers of fine-grained sulfate (mostly barite) with more porous layers of sulfate (anhydrite > barite), fringed by pyrite (Fig. 4C). Anhydrite comprises a large proportion of the samples collected in 1997. Samples collected in 1998 contain less anhydrite, and crystals examined by SEM show evidence of dissolution (Fig. 6A). The rare zinc sulfide crystals found in sulfate samples collected in 1998 are rounded and possibly abraded, suggesting that they partially dissolved and were transported (Fig. 6B). Silica was detected only in a few samples, where it forms minute (~2–5 μm) hemispherical protuberances that line cavities of microchannels (Fig. 6C).

The stainless steel sampling tube of an Osmo-Sampler deployed in the vents was partially dissolved (Fig. 7A) by the strongly acidic vent fluids (pH < 5, Sedwick *et al.* 1992). Deposits of euhedral crystals of barite (Fig. 7B) line the inside of the sampler. Botryoidal masses deposited on the outside (Fig. 7C) consist mostly of metallic Cr and Fe alloy, most likely derived from the dissolved metal tube.

Geochemistry

Bulk compositions of pieces of the hydrothermal mounds are given in Table 2, and results of electron-microprobe analyses of barite and anhydrite are given in Table 3. Representative compositions of iron and zinc sulfide are given in Tables 4 and 5, respectively. Bulk compositions are highly variable, depending on the heterogeneity of the samples. Some samples contain a significant amount of volcanic glass, reflected in the SiO_2 content. One sample, with SiO_2 as high as 50.4% (336–SC7F), is a siltstone criss-crossed by veins of sulfate. A Ba content of 11.7% indicates that barite comprises a significant part of the rock (Table 2). The sample with the highest CaO content (25.3%, 341–SC9A) contains the largest amount of anhydrite. The highly variable amounts of metallic elements reflect the erratic distribution of sulfide minerals (Table 2). Zn and Cd range from 118 to 11,500 ppm and 4.2 to 1740 ppm, respectively. Cu, although generally present in lower concentrations, also varies by an order of magnitude, ranging from 60 to 650 ppm. Pb is also highly variable, ranging from about 5 to 1380 ppm (Table 2).

Electron-microprobe analyses

Pyrite, the most abundant sulfide, contains only traces of Co (0.05–0.28%); Mn, As, and Sb are below detection limits. Zn and Cu are also typically near detection limits (Table 4), but rare crystals have up to 0.41% and 0.65%, respectively. Pb also is typically below detection limits, but concentrations as high as 2.95% were detected as a result of minute inclusions of Pb-rich minerals. Mn, Cu, As, and Pb in pyrrhotite are consistently below detection limits, but Co is present in trace amounts (0.10–0.15%). Zn was detected in only one sample at 0.38%. The zinc sulfide crystals typically are iron rich, but with low concentrations of Mn (0–

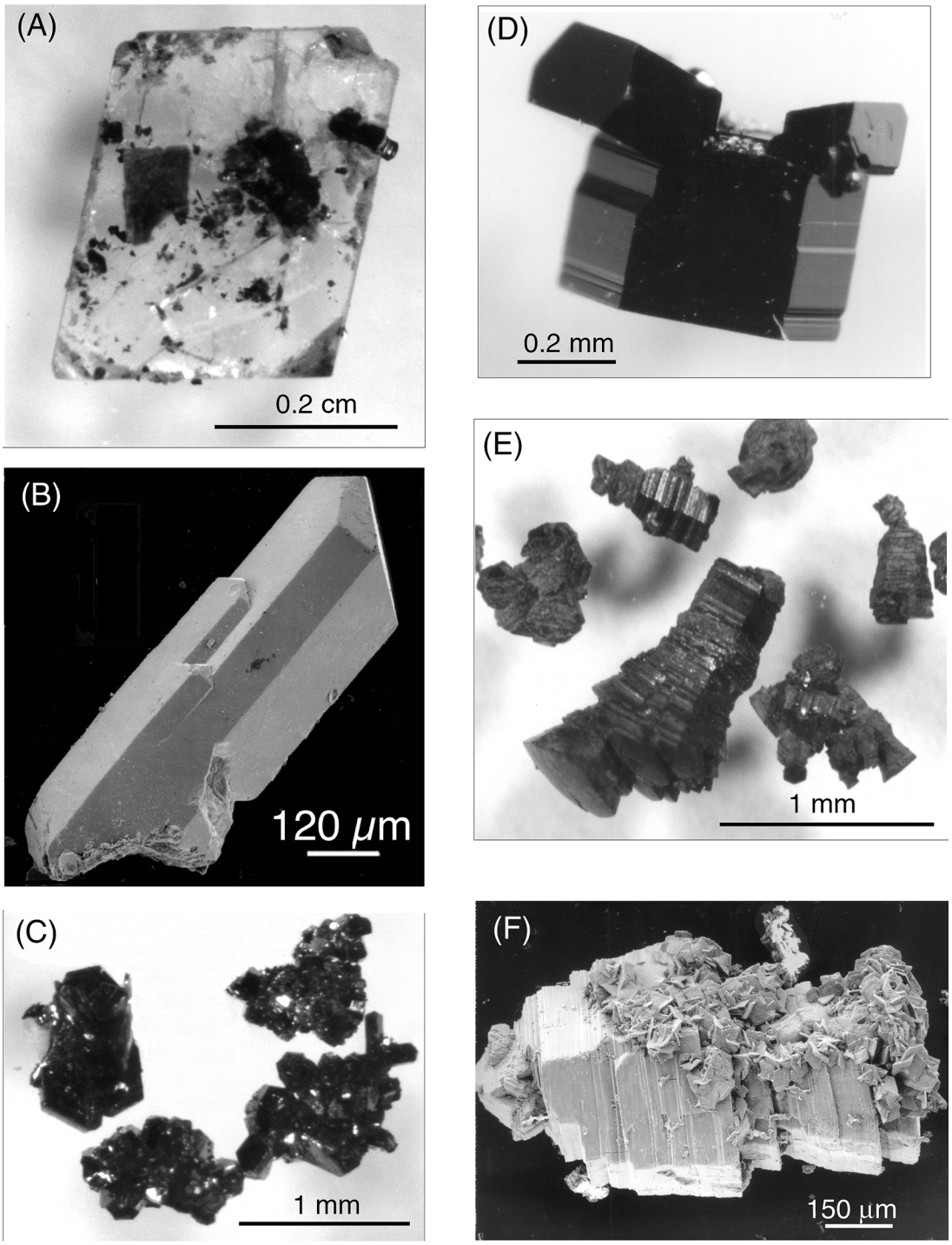

FIG. 3. A. Photomicrograph of tabular crystal of barite with zinc and iron sulfide inclusions. B. Scanning electron microscope (SEM) image of doubly terminated, elongate crystal of barite. Photomicrographs of pyrrhotite (C) and zinc sulfide (D, E) crystals. F. SEM image of Zn sulfide, covered by overgrowth of minute crystals of barite and pyrite.

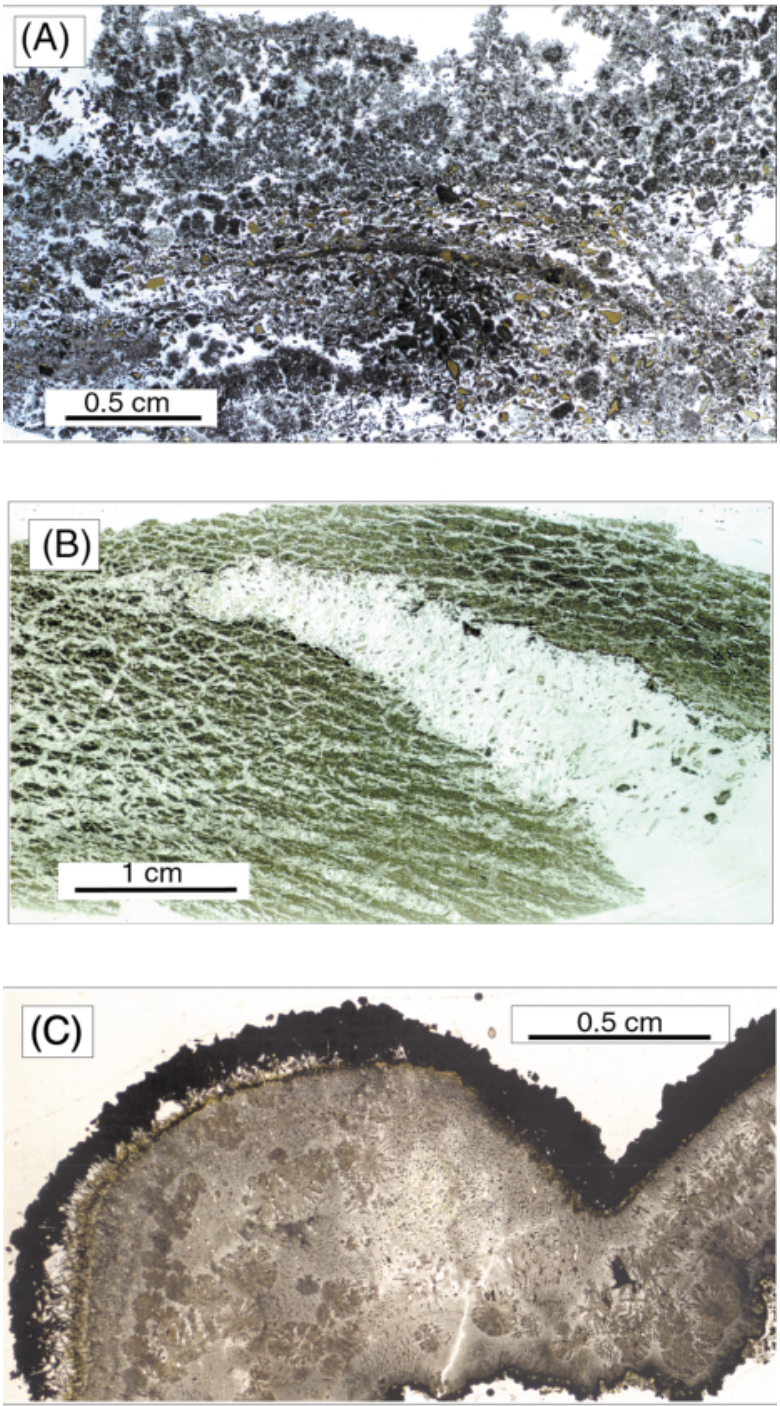

FIG. 4. Photomicrographs of thin sections of (A) sulfate precipitate enclosing fragments of brown volcanic glass, and (B) fine silt intruded and displaced by sulfate veinlets. The broader vein consists mostly of anhydrite. (C) Barite-rich sulfate collected from the mounds in 1998 shows concentric layers of sulfate, fringed by pyrite (black).

0.30%). The proportion of Fe varies from ~1.5 to over 15%. Co and As are consistently at or below detection limits. However, Cu, Pb, and Cd, although typically at or below detection limits, were present in considerable amounts in some samples (Table 5). The negative correlation between Cd and Zn concentration suggests the presence of a solid solution between ZnS and CdS. Small reddish inclusions in some Zn sulfide contain from 0.7 to 17.5% Cu, but only one larger inclusion is stoichiometric chalcopyrite (Table 5, Fig. 8A). Other minute, gray inclusions have high Pb (to 7.4%) and high Cd (to 14.0%, Fig. 8B) contents. Typically, analytical

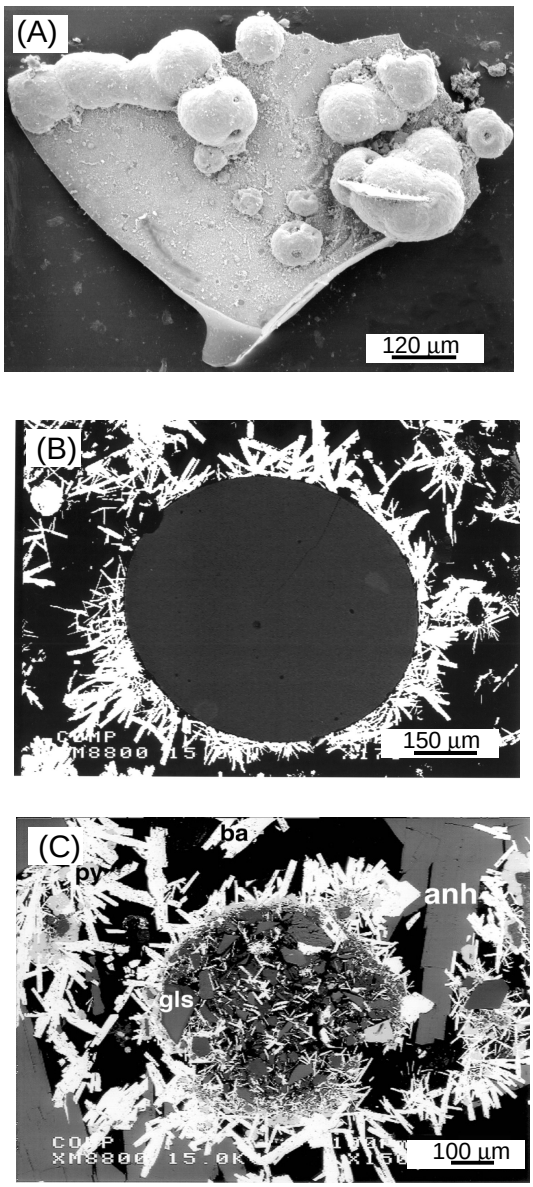

FIG. 5. Glass fragments generated during explosive submarine eruptions. A. SEM image of bubble-wall glass fragment (limu o' Pele) covered with Zn and Fe sulfide. B. Back-scattered-electron (BSE) image of glass sphere surrounded by delicate crystals of barite. C. BSE image of sphere of agglutinated, angular fragments of glass cemented and surrounded by sulfate and sulfide.

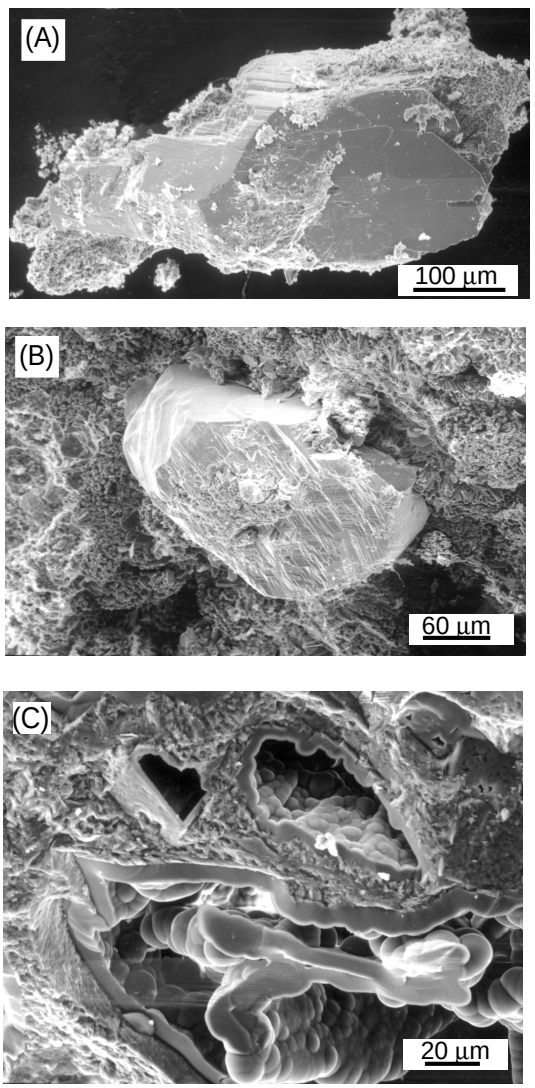

FIG. 6. SEM images of partly dissolved crystal of anhydrite (A), rounded, acid-etched Zn sulfide crystal showing evidence of dissolution (B) , and microchannels in sulfate precipitate that are lined with hemispherical silica along the interior and with botryoidal Fe sulfide on the outer surfaces (C).

totals of these particles, as well as of some of the Cu-rich inclusions, do not sum to 100%.

The barite crystals invariably contain significant amounts of Sr, but a large range (1.3 to 11.9%) is observed even for adjacent crystals. Although Sr in adjacent crystals could be highly variable, the large crystals collected in the sediment in 1996 are typically homogeneous. Barite crystals from the hydrothermal mounds, in contrast, show pronounced bands of compositional zoning with respect to Sr (Fig. 8C, Table 3). Sr is also present in low concentrations in the anhydrite (0.15 to 0.78%). In many cases, the analyses of anhydrite of samples collected in 1998 do not sum to 100%, apparently because crystals were hydrated to varying degrees.

TABLE 2. BULK COMPOSITION OF HYDROTHERMAL SAMPLES, LOIHI SEAMOUNT, HAWAI'I

Sample	1	2	3	4	5	6	7	8	9
					Fusion ICP (wt.%)				
SiO_2	14.04	1.87	7.03	6.63	2.56	50.39	24.99	1.27	35.41
Al_2O_3	3.72	0.45	1.34	1.15	0.56	6.44	4.18	0.11	6.89
Fe_2O_3	4.54	1.96	3.98	2.55	7.71	5.35	6.46	6.75	11.01
MnO	0.03	-0.01	0.01	0.01	-0.01	0.05	0.05	-0.01	0.11
MgO	3.56	0.28	0.51	0.52	0.30	2.11	2.88	0.04	8.11
CaO	25.26	0.48	0.99	0.83	2.17	2.82	2.61	0.17	5.54
Na_2O	1.00	0.08	0.11	0.29	0.12	0.40	1.08	0.07	1.28
K_2O	0.22	0.06	0.16	0.08	0.05	0.47	0.33	0.05	0.37
TiO_2	0.87	0.10	0.18	0.20	0.10	1.15	0.72	0.01	1.37
P_2O_5	0.11	-0.01	0.23	-0.01	-0.01	0.06	-0.01	-0.01	0.08
LOI	13.47	1.69	3.08	2.74	5.47	6.89	6.74	4.54	7.69
					LECO (wt.%)				
S	16.1	15.1	15.2	14.4	19.3	5.1	10.2	18	6.4
SO_4	49.2	40.6	35.8	36.7	38.3	10.6	5.75	4.45	3.80
					Fusion ICP (ppm)				
Cd	4.2	756	390	1740	234	67.1	301	213	214
Zn	118	3553	4973	11476	2919	2013	5181	2153	4009
					ICP–MS (wt.%)				
Ba	0.28	45.8	39.2	43.3	40.1	11.7	28.5	48.3	12.7
Sr	0.23	2.03	2.96	1.98	2.5	0.62	1.23	2.49	0.83
					ICP–MS (ppm)				
V	101	16	24	27	15	147	50	-5	184
Cr	276	37	80	75	45	304	335	-20	1020
Co	30	15	14	19	29	26	25	7	71
Ni	77	36	57	39	85	104	139	16	327
Cu	60	529	551	650	276	205	258	290	244
Zn	84	3620	4930	10500	3010	1950	5130	2020	3700
Ga	7	2	6	7	2	11	10	2	13
As	-5	-5	30	12	35	55	16	18	8
Rb	3.8	1	4.2	2.5	0.8	15	10	-2	9
Y	6.2	4.6	4.8	5.1	4.2	8.8	7.3	1.6	12
Zr	40	6.7	9.1	10	6	66	44	2	78
Nb	6.8	0.9	1.3	1.6	0.9	9	4.4	-0.5	8.9
Mo	3.2	2.9	107	27	8	79	302	59	46
Ag	-0.5	0.8	32	4	6.5	6.7	33	62	19
Sb	1	3.4	72	31	16	95	111	34	24
Pb	5	75	1261	343	674	1049	1380	325	118
Th	0.4	0.07	0.11	0.12	0.07	0.58	1.13	0.28	0.82
Tl	0.08	0.27	3.5	1.32	3.07	6.95	12	3.9	8.24
La	6.5	10.4	3.4	7.5	5.6	8.4	5.5	4	9.5
Ce	13	6.87	3.1	5.28	3.74	16	6.90	1.60	14
Pr	2.26	0.99	0.85	0.94	0.77	2.36	1.35	0.16	2.73
Nd	9.76	4.79	4.2	2.88	2.73	11.4	5.35	0.4	10.6
Sm	1.9	0.17	0.25	0.27	0.18	1.8	0.78	-0.2	2.17
Tb	0.26	-0.05	-0.05	-0.05	-0.05	0.31	0.22	0.03	0.43
Dy	1.38	0.22	0.32	0.42	0.25	1.35	1.2	0.1	2.35
Yb	0.54	0.09	0.1	0.12	0.09	0.72	0.46	-0.01	0.92
Lu	0.08	-0.01	-0.01	-0.01	-0.01	0.1	0.048	-0.002	0.114

Identity of the samples: 1: 341SC9A, 2: 341SC9B, 3: 340-R2, 4: 341-R2, 5: 336-R2, 6: 336SC7F, 7: 398M11, 8: 398SC4B, 9: 403SC5.

TABLE 3. REPRESENTATIVE RESULTS OF ELECTRON-MICROPROBE ANALYSES OF BARITE AND ANHYDRITE, LOIHI SEAMOUNT, HAWAI'I

Sample	BaO	SrO	CaO	FeO	SO_3	Total
			Barite			
P5-316SC2	49.84	11.85	n.d.	0.14	37.52	99.40
P5-336 R2	61.44	4.03	0.56	0.11	33.31	99.45
P5-341R2	62.78	3.57	0.17	0.00	34.43	100.94
P5-341SC9	59.86	5.46	0.19	0.00	34.99	100.50
P5-398M11	55.54	7.28	1.27	0.02	35.80	99.91
P5-398M11	63.97	1.23	0.03	0.00	34.21	99.44
P5-398SC1	52.13	10.74	1.40	0.08	36.15	100.50
			Anhydrite			
P5-336 SC7	0.00	0.28	45.67	0.00	53.36	99.31
P5-336 R2	0.21	0.36	44.89	0.09	53.92	99.48
P5-403M15	0.02	0.16	43.12	0.00	54.26	97.56
P5-398SC2	0.09	0.15	41.50	0.12	56.03	97.89

n.d.: not determined. All values are in weight percent.

TABLE 4. REPRESENTATIVE RESULTS OF ELECTRON-MICROPROBE ANALYSES OF IRON SULFIDE, LOIHI SEAMOUNT, HAWAI'I

Sample	S	Fe	Co	Cu	Zn	Pb	Total
			Pyrite				
P5-316SC2	53.49	46.15	0.05	0.03	0.02	0.00	99.78
P5-336 SC7	52.67	45.66	0.09	0.49	0.00	0.00	98.93
P5-336 SC7	53.29	44.88	0.13	0.51	0.00	0.00	98.89
P5-336 SC8	52.89	46.06	0.07	0.20	0.04	0.00	99.28
P5-336 SC9	52.90	45.94	0.10	0.01	0.00	0.00	98.96
P5-340 SC2	53.62	45.83	0.13	0.06	0.02	0.00	99.67
P5-341 R2	53.71	43.43	0.10	0.03	0.11	1.98	99.38
P5-341 SC1	53.56	45.98	0.08	0.07	0.00	0.00	99.68
P5-341 SC1	39.41	58.59	0.13	0.04	0.00	0.00	98.17
P5-341 SC1	39.58	58.89	0.13	0.03	0.07	0.00	98.72
P5-341 SC8	39.54	58.29	0.15	0.04	0.00	0.00	98.02
			Pyrrhotite				
P5-341SC9B	53.10	44.63	0.13	0.21	0.03	0.83	98.93
P5-341R2	53.20	46.06	0.06	0.02	0.05	0.39	99.81

Mn, As, Sb: below detection limits. All values are in weight percent.

TABLE 5. REPRESENTATIVE RESULTS OF ELECTRON-MICROPROBE ANALYSES OF ZINC AND COPPER SULFIDE, LOIHI SEAMOUNT, HAWAI'I

Sample	S	Fe	Co	Cu	Zn	Pb	Mn	Cd	Total
				Zn-rich phase					
P5-316SC2	34.03	14.56	0.04	0.03	51.55	0.00	0.16	n.d.	100.37
P5-340SC1-2	34.28	8.94	0.06	0.01	57.37	0.00	0.11	0.00	100.76
P5-340SC2-1	34.14	12.35	0.05	0.01	52.85	0.00	0.30	0.00	99.70
P5-340SC2-3	34.06	9.12	0.02	0.03	56.21	0.00	0.06	0.00	99.50
P5-340SC2-8	33.88	8.63	0.03	0.03	57.40	0.00	0.06	0.00	100.03
P5-341SC9B	31.16	1.75	0.00	0.00	53.29	0.00	0.00	12.39	98.60
P5-341 R2-1	31.33	1.34	0.00	0.00	50.88	0.00	0.04	14.04	97.63
P5-341 R2-2	32.75	1.72	0.02	1.06	59.94	0.50	0.02	2.94	98.98
				Cu-rich phase					
P5-340SC1-1	34.73	30.25	0.00	32.02	1.21	0.00	0.00	0.00	98.23
P5-340SC1-2	35.15	31.00	0.00	31.81	1.80	0.00	0.00	0.00	99.75

As, Sb: below detection limits. All measurements in weight percent.

Isotopic Composition

Sulfur isotopic compositions of sulfide and sulfate minerals are given in Tables 6 and 7, respectively. The sulfide minerals have a narrow range of negative $\delta^{34}S$ values, ranging from –2.17 to –0.3‰. The isotopic values of all of the sulfides measured are less than 0‰ CDT (av. –1.1‰; Fig. 9), and are consistently lower than the bulk $\delta^{34}S$ of ocean-floor basalt (+0.3‰; Sakai *et al.* 1984). The barite and anhydrite, calibrated against the IAEA standards, have $\delta^{34}S$ values of about 21.9 ± 0.3‰. Standard NBS–127, which was precipitated from seawater sulfate, gave a value of 22.60‰, very close to the newly defined value of IAEA–S3 (Ding *et al.* 2001). IAEA–S3 formerly had an assumed value of 21‰, identical to the $\delta^{34}S$ value of seawater sulfate determined by Rees *et al.* (1978). Comparison of older data on seafloor sulfates with the data presented here, calibrated relative to the newly established value for IAEA–S3, makes it appear that the sulfates from Loihi are isotopically enriched relative to seawater sulfate and previously measured anhydrite from hydrothermal vents. In fact, the Loihi sulfates are on average depleted in ^{34}S by approximately 0.6‰ relative to seawater sulfate, similar to previously analyzed hydrothermal vent sulfates.

The $^{87}Sr/^{86}Sr$ compositions of barite range from 0.70420 to 0.70456 ± 2 (Table 7), values that are intermediate between seawater (0.7091) and Loihi basalt (0.7034 to 0.7037: Staudigel *et al.* 1984), requiring a basaltic component.

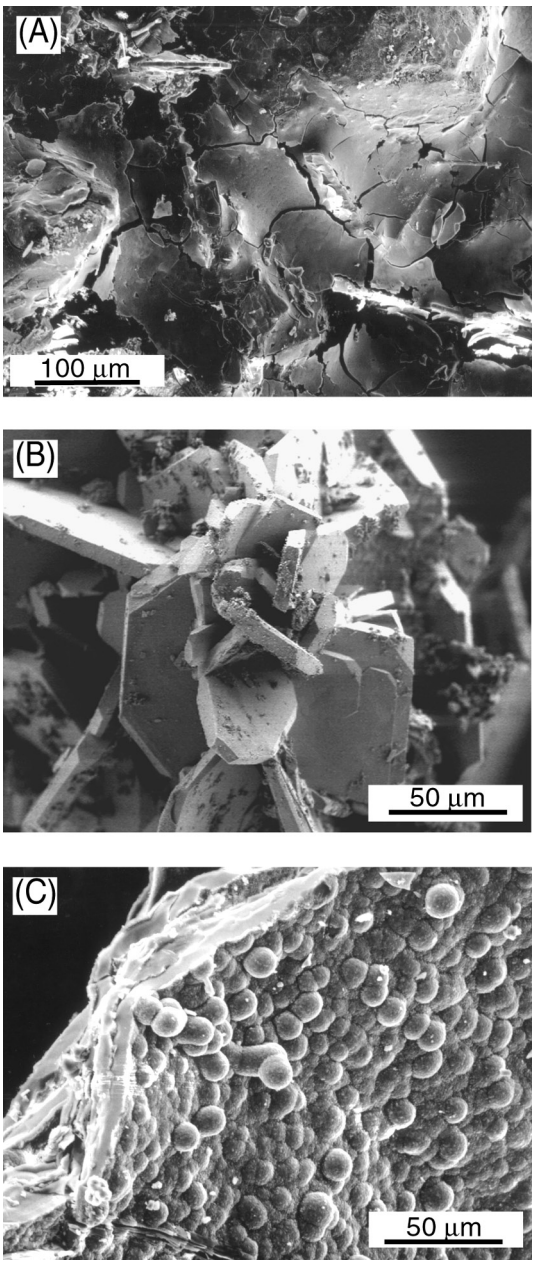

FIG. 7. SEM images of corroded stainless steel tube of Osmo sampler (A), barite crystals lining interior of sampler (B), and Cr-rich masses deposited on outside of sampler (C).

TABLE 6. SULFUR ISOTOPE VALUES OF SULFIDE MINERALS, LOIHI SEAMOUNT, HAWAI'I

Sample	Mineral	$\delta^{34}S$
P5–340SC2	Pyrrhotite	–0.30
P5–340SC2	Sphalerite	–0.82
P5–340SC2	Wurtzite	–0.52
P5–340SC2–1	Pyrite	–0.84
P5–340SC2–2	Pyrite	–1.41
P5–341SC1–1	Wurtzite	–0.89
P5–341SC1–2	Wurtzite	–1.09
P5–341SC1–3	Wurtzite	–1.07
P5–341SC1–4	Wurtzite	–1.19
P5–341SC8	Pyrrhotite	–0.84
P5–341SC8–1	Wurtzite	–1.33
P5–341SC8–2	Wurtzite	–2.17
P5–341SC8–1	Chalcopyrite	–1.12
P5–341SC8–2	Chalcopyrite	–1.48

Values of $\delta^{34}S$ are expressed in ‰.

TABLE 7. SULFUR AND STRONTIUM ISOTOPE VALUES OF SULFATE MINERALS, LOIHI SEAMOUNT, HAWAI'I

Sample	Mineral	$\delta^{34}S$	$^{87}Sr/^{86}Sr$ *
P5–316 SC2	Barite	21.81	0.704307 ± 16
P5–336SC7	Anhydrite	21.47	n.d.
P5–340SC2	Barite	22.25	0.704563 ± 14
P5–341SC1	Barite	21.98	0.704374 ± 10
P5–341SC8	Barite	22.27	0.704195 ± 21

* barite crystals were leached in 2.5 N HCl at 125°C for 3 weeks; n.d.: not determined. Values of $\delta^{34}S$ are expressed in ‰.

Discussion

The 1996 collapse event

The seismic events leading to the collapse of the summit profoundly modified the hydrothermal system. The sudden collapse of the summit crater brought large volumes of seawater in contact with hot rocks or magma (or both). The change from low-temperature diffuse venting to high-temperature discharge of hydrothermal fluids probably occurred in the form of a cataclysmic megaplume. The shape of fresh glass shards, encased and cemented by sulfide and sulfate crystals (Fig. 5), suggests explosive ejection into the water column. Observations of limu o Pele formed on mid-ocean ridges at pressures greater than the critical point of seawater led Clague *et al.* (2003a) to conclude that explosive eruptions could be driven by release of magmatic volatiles (mainly CO_2). The presence of limu o Pele, Pele's hair, and glass spheres in volcanic sands collected on Loihi are evidence for similar pyroclastic eruptions (Clague *et al.* 2003b). The glass particles in the sulfate samples may have originated in a small-volume phreatomagmatic eruption associated with the collapse of the summit. Alternatively, the cataclysmic venting may have resuspended glass particles ejected during previous pyroclastic eruptions on Loihi. The wide compositional range of the glass fragments supports this interpretation. In addition, no new lava flow was discovered during the Rapid Response Cruise in 1996. On the basis of these observations, the summit collapse was inferred to be strictly a tectonic event, possibly due to magma withdrawal as a result of an eruption or dike injection deep on the rift zone (Loihi Science Team 1997, Davis & Clague 1998). These two scenarios are not mutually exclusive. A small volume of lava may have erupted as fragmental material, but not enough was present to result in a flow, or any newly erupted material may have been covered or destroyed by the collapse. The fresh appearance of the glass suggests that it was not in prolonged contact with hydrothermal fluids.

Origin of sulfide minerals

Besides fresh glass fragments, the hydrothermal plume injected large amounts of bacterial floc, magmatic gas, including ^{3}He, rock powder, and hydrothermal precipitates from the subsurface into the water column (Loihi Science Team 1997). The presence of wurtzite, chalcopyrite, and pyrrhotite suggests fluid temperatures above 250°C (Craig & Scott 1974). Water temperatures in excess of 300°C have been measured at black smoker vents of mid-ocean ridges (*e.g.*, Hannington *et al.* 1995, Von Damm 1995, and references therein), where similar assemblages of minerals are common. Although crystal aggregates and sulfide coatings on rock fragments are abundant, no hydrothermally altered ba-

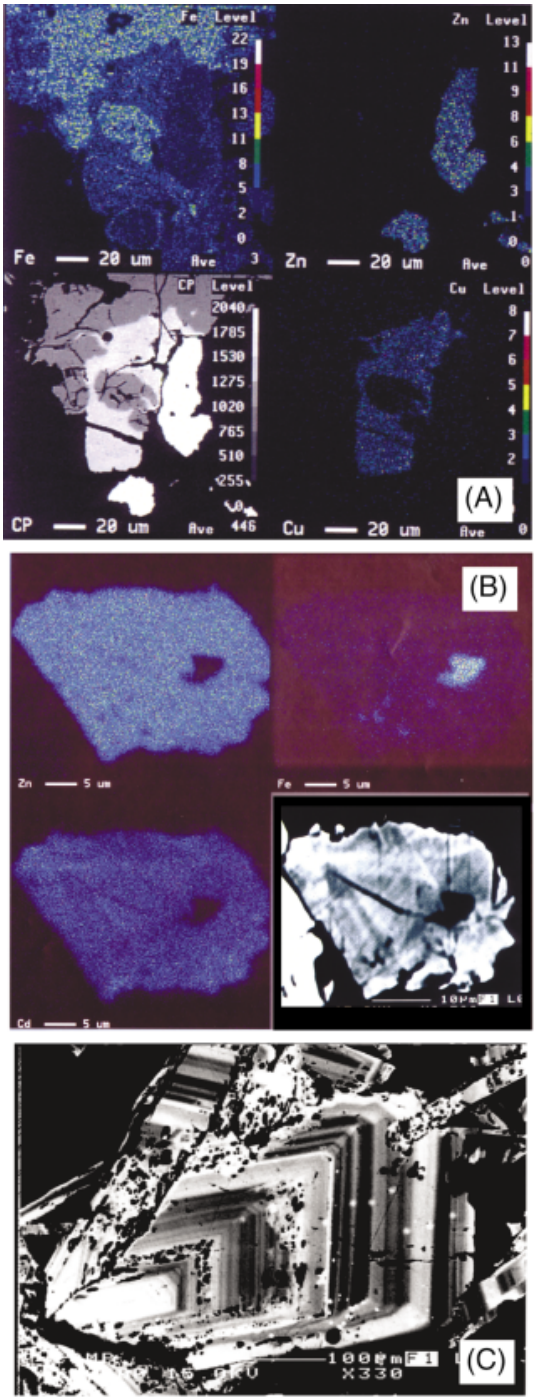

FIG. 8. A. X-ray images of distribution of Fe, Zn, and Cu for BSE image shown in lower left corner. B. X-ray images of the distribution of Zn, Cd, and Fe for BSE image shown in the lower right corner. C. BSE image shows compositionally zoned barite. Darker bands are rich in Sr.

salt, or veined greenstones, resembling subsurface stockwork was observed.

After the initial cataclysmic discharge of high-temperature fluids, lower-temperature fluids built the barite-rich mounds. Measured temperatures of up to 200°C (Wheat *et al.* 2000) are considerably higher than those observed over many years (<30° C, *e.g.*, DeCarlo *et al.* 1983, Malahoff *et al.* 1982) prior to the seismic events. In order to build the mounds, venting must have also been somewhat channeled locally, and less diffuse than previously observed. The sulfide mineral precipitated with the sulfate in the barite-rich mounds appears to be all pyrite. The high-temperature sulfide phases (*e.g.*, wurtzite, chalcopyrite, pyrrhotite) apparently were ejected only during the initial hot-plume discharge. In contrast to the unoxidized sulfide crystals collected in 1996, extensive iron oxide cover on all pyrrhotite and zinc sulfide crystals found in the sediment in subsequent years indicates that these crystals had resided there for some time. The dissolution features on some crystals of zinc sulfide (Fig. 6B) suggest that these minerals do not survive very long, which may explain why they had not been reported previously. The homogeneous composition of the large, euhedral crystals of sulfide and sulfate suggests that no further reaction with hydrothermal fluids occurred after rapid ejection by the plume. In contrast, the barite crystals found in the porous mounds show strong compositional zoning (Fig. 8C). Oscillatory zoning in barite–celestine solid solutions has been produced experimentally (Putnis *et al.* 1992), but owing to the significant difference in ionic radius between Ba^{2+} and Sr^{2+}, natural occurrences of intermediate compositions of $(Ba,Sr)SO_4$ appear to be rare (Tekin *et al.* 2002). Large variations in Sr contents in zoned crystals of barite and in single crystals found in close proximity to each other probably reflect fluctuations in temperature and composition of the vent fluids.

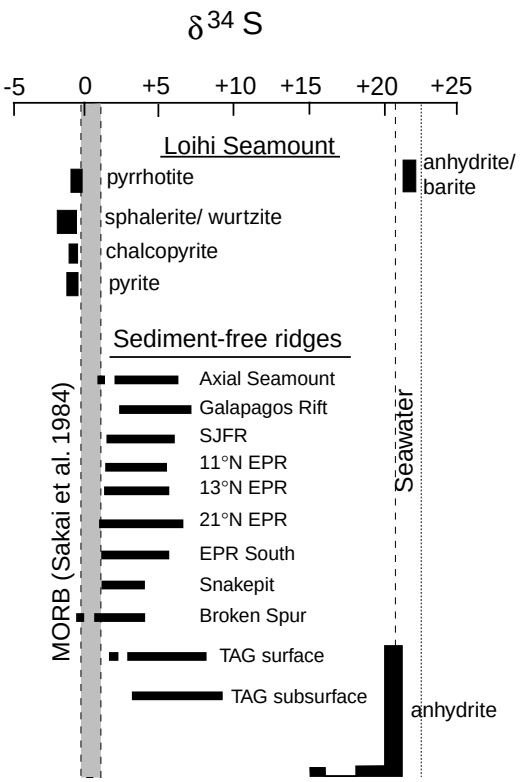

FIG. 9. Sulfur isotopic ratio of Loihi sulfide have a distinctly negative $\delta^{34}S$ value compared with those from sediment-free spreading centers. Negative values, observed for many sediment-hosted sulfide deposits, result from incorporation of sulfide formed by bacterially mediated reduction of sulfate. Data for mid-ocean ridge sulfide are from Herzig *et al.* (1998). Dashed line represents seawater sulfate, after Rees *et al.* (1978); dotted line is the value for seawater sulfate (NBS–127) obtained using the redefined value for the IAEA–3 sulfur isotope standard (Ding *et al.* 2001). Modified from Herzig *et al.* (1993) and Goodfellow & Blaise (1988).

Comparison with mid-ocean ridge deposits

Hydrothermal deposits, resulting from the interaction of heated seawater with oceanic crust, have been extensively studied at numerous spreading centers. Major controls on sulfide deposition include the temperature, pH, activity of sulfur, $a(S_2)$, and fugacity of oxygen, $f(O_2)$ of the fluids (*e.g.*, Hannington *et al.* 1995, and references therein). The initial formation of a hydrothermal deposit on a spreading center may start with release of a megaplume of hot fluids similar to what happened on Loihi. On a fast-spreading center with a long-lived source of heat and easy access of seawater along faults and fractures because of a greater rate of extension, large hydrothermal deposits can grow with time. The hydrothermal system on an oceanic volcano probably more closely resembles that of a slow-spreading center that also has infrequent eruptions. Larger structures, such as those observed at the TAG hydrothermal field at the Mid-Atlantic Ridge (Kleinrock & Humphris 1996) and the Seacliff hydrothermal site on the northern Gorda Ridge (Clague & Rona 1990), probably require structural control in the form of faults and fissures to allow flow to be more focused. Chimneys composed predominantly of anhydrite are more fragile than those predominantly composed of sulfide, and appear to be more easily eroded (*e.g.*, Middle Valley, Ames *et al.* 1993). Building exceptionally large structures, like those at the Endeavour Ridge (Robigou *et al.* 1993), appears to be due to precipitation of silica. The low pH (<5) of the Loihi fluids is not conducive to precipitation of silica in the absence of significant conductive cooling of the fluids (Janecky & Seyfried 1984),

and silica is observed in the deposits only in minute quantities.

The composition of hydrothermal minerals is highly variable among hydrothermal deposits and even from a single chimney (*e.g.*, Hannington *et al.* 1995, and references therein, Goodfellow & Franklin 1993, Zierenberg *et al.* 1993). Compositional variability in a chimney reflects the fluctuations in temperature and composition of the vent fluids (*e.g.*, Hannington *et al.* 1995, and references therein). Systematic differences between black and white smokers primarily reflect temperature differences that control the metal content of fluids. The barite-rich mounds on Loihi more closely resemble white smoker deposits at mid-ocean ridges, with respect to mineralogy and chemistry. The sulfide particles ejected during the seismic event are identical to minerals found in black smokers. The composition of iron and zinc sulfide is similar to that of the same phases from hydrothermal systems at spreading centers. The iron content of Zn sulfide is relatively high compared to that reported from sediment-free mid-ocean ridges (MOR), indicating that the fluids had lower $a(S_2)$ than typical MOR sulfide deposits (Scott & Kissin 1973). The relative proportions of Cu, Zn, and Pb (Fig.10) in the Loihi sulfides indicate slightly higher amounts of Pb, and barite is slightly higher in Sr compared to that observed for sediment-free ridges (*e.g.*, Goodfellow & Franklin 1993). Similar or higher values are not uncommon in comparable phases from sediment-covered ridges (Goodfellow & Blaise 1988, Peter & Scott 1988); however, the Loihi basalt (Garcia *et al.* 1995) also contains higher concentrations of these elements than MORB (White *et al.* 1997).

Although mineral and bulk compositions are not significantly different, the isotopic composition of the Loihi sulfides is distinct from MOR hydrothermal deposits. A review of sulfur isotope values from mid-ocean ridge hydrothermal deposits (Shanks 2001) shows that they are all enriched in ^{34}S relative to ocean-floor basalts (Sakai *et al.* 1984). Among 550 analyses of sulfur isotopes from mid-ocean ridges, only one has a $\delta^{34}S$ value less than 0‰ (Herzig *et al.* 1998). The slight enrichment in ^{34}S relative to magmatic sulfur, which is typical of MOR hydrothermal deposits, results from incorporation of minor amounts of reduced seawater sulfate in these systems (Woodruff & Shanks 1988). Sulfides from sediment-covered ridges may incorporate sulfide derived by bacterial sulfate reduction, and negative sulfur isotope values are commonly observed (Peter & Shanks 1992). All of the Loihi sulfide minerals, including single crystals of hexagonal pyrrhotite, wurtzite, and chalcopyrite interpreted to have formed at high temperature, have

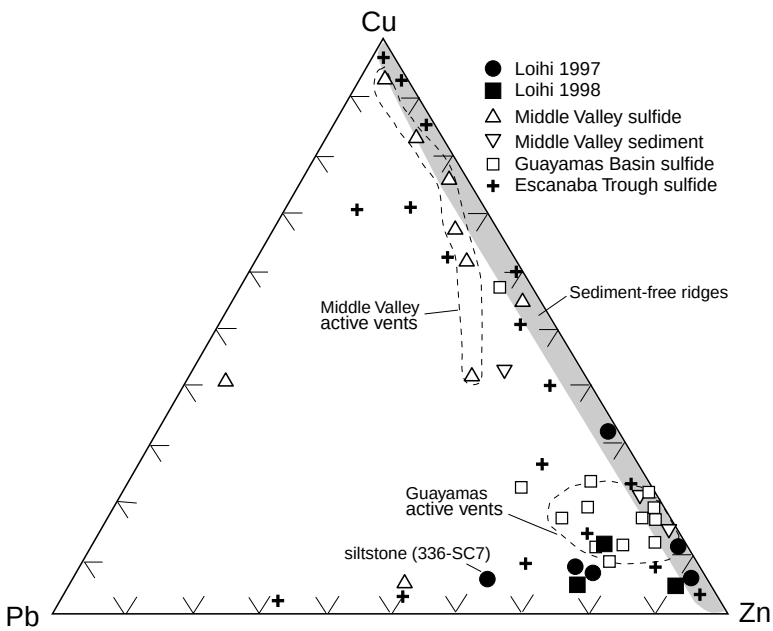

FIG. 10. Proportions of Pb, Cu and Zn in compositions of bulk samples from Loihi compared to those from spreading centers (modified from Ames *et al.* 1993). Data for hydrothermally altered sediment from Middle Valley from Goodfellow & Blaise (1988). Although proportions of these elements are similar, actual concentrations are several times greater in massive sulfide deposits from mid-ocean ridges.

negative sulfur isotope values. We do not think that the negative sulfur isotope values are caused by incorporation of biogenic sulfide, but suggest instead that they represent derivation from basalt that has degassed SO_2. High-temperature hydrothermal sulfide minerals with negative isotope values have also been reported from the Lau back-arc basins, which Herzig *et al.* (1993) interpreted as evidence for disproportionation of magmatic SO_2.

Analysis of Loihi glass show that many samples have low sulfur contents (600–900 ppm) relative to undegassed basalt despite eruption at depths greater than 1000 m (Clague *et al.* 2000, 2003b), consistent with partial loss of sulfur during vesiculation and eruption. Wallace & Carmichael (1992) showed that at the $f(S_2)$ and $f(O_2)$ values calculated for Loihi basalts, sulfur would be lost as SO_2. Any SO_2 lost through vesiculation would be enriched in ^{34}S relative to average basaltic sulfur (Sakai *et al.* 1984), leaving behind isotopically depleted sulfur with values below 0.3‰, depending on the extent of degassing. We suggest that the negative sulfur isotope values observed from hydrothermal sulfides are consistent with derivation of sulfur by water–rock interaction with partially degassed basalt.

It is highly unlikely that the hydrothermal mounds on Loihi will grow to a significant height because the highly porous layers of volcaniclastite on Loihi favor diffuse venting and subseafloor mixing of hydrothermal fluids (Wheat *et al.* 2000). The fragile nature of the mounds, the dissolution of anhydrite and sulfide phases, combined with slope instability of the seamount's flank, also make it unlikely that such deposits survive intact in the geological record. Undoubtedly, high-temperature sulfide minerals were ejected during previous hydromagmatic eruptions (Clague *et al.* 2003b), and future hydromagmatic eruptions that may accompany collapse events are likely to do so again. On submarine, ocean-island volcanoes, hydrothermal mineral deposits are probably formed and destroyed many times during the volcano's evolution.

Conclusions

High-temperature sulfide minerals were ejected by a hydrothermal megaplume at Loihi Seamount during the collapse of the summit, following the seismic events in the summer of 1996. This is the first documented occurrence of a high-temperature hydrothermal system on an ocean island volcano. Phases such as chalcopyrite and wurtzite confirm the presence of high-temperature fluids in the hydrothermal system that, prior to these events, discharged only low-temperature (<30°C) fluids. Mineral compositions of sulfide and sulfates collected after these events are similar to those of comparable hydrothermal phases from spreading centers. However, the negative sulfur isotopic values of the sulfides are unique from a sediment-free environment, indicating an origin from basalt that has lost magmatic SO_2 with little to no contribution from reduced seawater sulfate. Sulfur isotopic values of sulfates closely match that of seawater. Oxidation and dissolution of high-temperature minerals observed in the two years following the event suggest that such deposits are not easily preserved in the geological record. Similar mineral deposition from hydrothermal plume events probably occurred repeatedly in the past and will do so in the future in response to periodic volcanic and tectonic activity.

Acknowledgements

We thank Frank Sansone and Gary McMurtry for their generous sharing of samples from their dives. We also thank T. Kirby and the staff of the Hawaii Undersea Research Laboratory for logistical support, and members of the science parties for helping with onboard handling of samples. Special thanks to T. Kirby for providing us with his artistic rendition of the vent sites used to construct Figure 1B. R. Oscarson and L. Calk assisted with scanning electron microscope and electron-microprobe analyses, respectively, and G. Czamanske provided sulfide standards. Helpful reviews by E. Mathez, D. Crowe, and Associate Editor E. Ripley improved the manuscript. This study was supported by the David and Lucile Packard Foundation.

References

Ames, D.E., Franklin, J.M. & Hannington, M.D. (1993): Mineralogy and geochemistry of active and inactive chimneys and massive sulfide, Middle Valley, northern Juan de Fuca Ridge: an evolving hydrothermal system. *Can. Mineral.* **31**, 997-1024.

Both, R., Crook, K., Taylor, B., Brogan, S., Chappell, B.W., Frankel, E., Liu, L., Sinton, J. & Tiffin, D. (1986): Hydrothermal chimneys and associated fauna in the Manus back-arc basin, Papua, New Guinea. *Trans. Am. Geophys. Union* (*Eos*) **67**, 489-490 (abstr.).

Clague, D.A., Batiza, R., Head, J.W., III & Davis, A.S. (2003b): Pyroclastic and hydrothermal deposits on Loihi Seamount, Hawaii. *In* Explosive Subaqueous Volcanism (J. White, J. Smellie & D. Clague, eds.). *Am. Geophys. Union, Monogr.* (in press).

_____, Davis, A.S., Bischoff, J.L., Dixon, J.E. & Geyer, R. (2000): Lava bubble-wall fragments formed by submarine hydrovolcanic explosions on Loihi Seamount and Kilauea Volcano. *Bull. Volcanol.* **61**, 437-449.

_____, _____ & Dixon, J.E. (2003a): Submarine strombolian eruptions on the Gorda mid-ocean ridge. *In* Explosive Subaqueous Volcanism (J. White, J. Smellie & D. Clague, eds.). *Am. Geophys. Union, Monogr.* (in press).

_____ & Rona, P.A. (1990): Geology of the GR14 site on northern Gorda Ridge. *In* Gorda Ridge: a Seafloor Spreading Center in the United States' Exclusive Economic Zone

(G.R. McMurray, ed.). Springer-Verlag, New York, N.Y. (31-50).

COUSENS, B.L. (1996): Magmatic evolution of Quaternary mafic magmas at Long Valley Caldera and the Devils Postpile, California: effects of crustal contamination on lithospheric mantle-derived magmas. *J. Geophys. Res*. **101**, 27,673-27,689.

CRAIG, J.R. & SCOTT, S.D. (1974): Sulfide phase equilibria. *In* Sulfide Mineralogy (P.H. Ribbe, ed.). *Rev. Mineral*. **1**, CS1-CS110.

DAVIS, A.S. & CLAGUE D.A. (1998): Changes in the hydrothermal system at Loihi Seamount after formation of Pele's pit in 1996. *Geology* **26**, 399-402.

DECARLO, E.H., MCMURTRY, G.M. & YEH, HSUEH-WEN (1983): Geochemistry of hydrothermal deposits from Loihi volcano, Hawaii. *Earth Planet. Sci. Lett*. **66**, 438-449.

DEGENS, E.T. & ROSS, D. (1969): *Hot Brines and Recent Heavy Metal Deposits in the Red Sea*. Springer Verlag, New York, N.Y.

DING, T.S., VALKIERS, S., KIPPHARDT, H., DE BIÈVRE, P., TAYLOR, P.D.P., GONFIANTINI, R. & KROUSE, R. (2001): Calibrated sulfur isotope abundance ratios of three IAEA sulfur isotope reference materials and V–CDT with a reassessment of the atomic weight of sulfur. *Geochim. Cosmochim. Acta* **65** 2433-2437.

FORNARI, D.J., GARCIA, M.O., TYCE, R.C. & GALLO, D.G. (1988): Morphology and structure of Loihi Seamount based on Seabeam sonar mapping. *J. Geophys. Res*. **93** 15,227-15,238.

GARCIA, M.O., FOSS, D.J.P., WEST, H.B. & MAHONEY, J.J. (1995): Geochemical and isotopic evolution of Loihi Volcano, Hawaii, *J. Petrol.* **36**, 1647-1674.

GOODFELLOW, W.D. & BLAISE, B. (1988): Sulfide formation and hydrothermal alteration of hemipelagic sediment in Middle Valley, northern Juan de Fuca Ridge. *Can. Mineral*. **26**, 675-696.

_____ & FRANKLIN, J.M. (1993): Geology, mineralogy, and chemistry of sediment-hosted clastic massive sulfides in shallow cores, Middle Valley, northern Juan de Fuca Ridge. *Econ. Geol*. **88**, 2037-2068.

HANNINGTON, M.D., JONASSON, I.R., HERZIG, P.M. & PETERSEN, S. (1995): Physical and chemical processes of sea floor mineralization at mid-ocean ridges. *In* Sea Floor Hydrothermal Systems: Physical, Chemical, Biological, and Geological Interactions (S.E. Humphris, R.A. Zierenberg, L.S. Mullineaux & R.E. Thomson, eds.). *Am. Geophys. Union, Monogr*. **91**,115-157.

HERZIG, P.M., HANNINGTON, M.D. & ARRIBAS, A., JR. (1993): Sulfur isotopic composition of hydrothermal precipitates from the Lau back-arc: implications for magmatic contributions to seafloor hydrothermal systems. *Mineral. Deposita* **33**, 226-237.

_____, PETERSEN, S., & HANNINGTON, M.D. (1998): Geochemistry and sulfur-isotopic composition of the TAG hydrothermal mounds, Mid-Atlantic Ridge, 26° N. *Proc. ODP, Sci. Results* **158**, 47-70.

HILTON, D.R., MCMURTRY, G.M. & GOFF, F. (1998): Large variations in vent fluid $CO_2/^3He$ ratios signal rapid changes in magma chemistry at Loihi Seamount, Hawaii. *Nature* **396**, 359-362.

IIZASA, K., YUASA, M. & YOKOTA, S. (1992): Mineralogy and geochemistry of volcanogenic sulfides from the Myojinsho submarine caldera, the Shichito–Iwojima Ridge, Izu–Ogasawara Arc, northwestern Pacific. *Mar. Geol*. **108**, 39-58.

JANECKY, D.R. & SEYFRIED, W.E., JR. (1984): Formation of massive sulfide deposits on oceanic ridge crests: incremental reaction models for mixing between hydrothermal solutions and seawater. *Geochim. Cosmochim. Acta* **48**, 2723-2738.

KARL, D.M., MCMURTRY, G.M., MALAHOFF, A. & GARCIA, M.O. (1988): Loihi Seamount, Hawaii: a mid-plate volcano with a distinctive hydrothermal system. *Nature* **335**, 532-535.

KLEINROCK, M.C & HUMPHRIES, S.E. (1996): Structural control on seafloor hydrothermal activity at the TAG active mound. *Nature* **328**, 149-153.

LOIHI SCIENCE TEAM (1997): Researchers rapidly respond to submarine activity at Loihi volcano, Hawaii. *Trans. Am. Geophys. Union* (*Eos*) **78**, 232-233 (abstr.).

MALAHOFF, A., MCMURTRY, G.M., WILTSHIRE, J.C., & YEH, HSUEH-WEN (1982): Geology and chemistry of hydrothermal deposits from active submarine volcano Loihi, Hawaii. *Nature* **298**, 234-239.

MOORE, J.G., CLAGUE, D.A. & NORMARK, W.R. (1982): Diverse basalt types from Loihi Seamount, Hawaii. *Geology* **10**, 88-92.

PETER, J.M. & SCOTT, S.D. (1988): Mineralogy, composition, and fluid-inclusion microthermometry of sea floor hydrothermal deposits in the southern trough of Guaymas Basin, Gulf of California. *Can. Mineral*. **26**, 567-587.

_____ & SHANKS, W.C., III (1992): Sulfur, carbon, and oxygen isotope variations in submarine hydrothermal deposits of Guaymas basin, Gulf of California. *Geochim. Cosmochim. Acta* **56**, 2025-2040.

PUTNIS, A., FERNANDEZ-DIAZ, L. & PRIETO, M. (1992): Experimentally produced oscillatory zoning in the (Ba, Sr)SO_4 solid solution. *Nature* **358**, 743-745.

REES, C.E., JENKINS, W.J. & MONSTER, J. (1978): The sulphur isotopic composition of ocean water sulfate. *Geochim. Cosmochim. Acta* **42**, 377-381.

ROBIGOU, V., DELANEY, J.R. & STAKES, D.S. (1993): Large massive sulfide deposits in a newly discovered active hydrothermal system, the High Rise Field, Endeavour segment, Juan de Fuca Ridge. *Geophys. Res. Lett.* **20**, 1887-1890.

SAKAI, H., DES MARAIS, D.J., UEDA, A. & MOORE, J.G. (1984): Concentrations and isotope ratios of carbon, nitrogen and sulfur in ocean-floor basalts. *Geochim. Cosmochim. Acta* **48**, 2433-2441.

_____, TSUBTA, H., NAKAI, T., ISHIBASHI, J., AKAGI, T., GAMO, T., TILBROOK, B., IGARASHI, G., KODERA, M., SHITASHIMA, K., NAKAMURA, S., FUJIOKA, K., WATANABE, M., MCMURTRY, G. MALAHOFF, A. & OZIMA, M. (1987): Hydrothermal activity on the summit of Loihi Seamount, Hawaii. *Geochem. J.* **21**, 11-21.

SCHOLTEN, J.C., STOFFERS, P., GARBE-SCHOENBERG, D. & MOAMMAR, M. (2000): Hydrothermal mineralization in the Red Sea. *In* Handbook of Marine Mineral Deposits (D.S. Cronan, ed.), CRC Press, New York, N.Y. (369-395).

SCOTT, S.D. & KISSIN S.A. (1973): Sphalerite composition in the Zn–Fe–S system below 300°C. *Econ. Geol.* **68**, 475-479.

SEDWICK, P.N., MCMURTRY, G.M. HILTON, D.R. & GOFF, F. (1994): Carbon dioxide and helium in hydrothermal fluids from Loihi Seamount, Hawaii, USA: temporal variability and implications for the release of mantle volatiles. *Geochim. Cosmochim. Acta* **58**, 1219-1227.

_____, _____ & MACDOUGALL, J.D. (1992): Chemistry of hydrothermal solutions from Pele's Vents, Loihi Seamount, Hawaii. *Geochim. Cosmochim. Acta* **56**, 3643-3667.

SHANKS, W.C., III (2001): Stable isotopes in seafloor hydrothermal systems: vent fluids, hydrothermal deposits, hydrothermal alteration, and microbial processes. *In* Stable Isotope Geochemistry (J.W. Valley & D.R. Cole, eds.). *Rev. Mineral. Geochem.* **43**, 469-525.

STAUDIGEL, H., ZINDLER, A., HART, S.R., LESLIE, T., CHEN, C.-Y. & CLAGUE, D.A. (1984): The isotope systematics of a juvenile intraplate volcano: Pb, Nd, and Sr isotope ratios of basalts from Loihi Seamount, Hawaii. *Earth Planet. Sci. Lett.* **69**, 13-29.

TEKIN, E., VAROL, B. & SAYILI, I.S. (2002): Indications of intermediate compositions in the $BaSO_4$–$SrSO_4$ solid-solution series from the Bahçeciktepe celestine deposit, Sivas, east-central Anatolia, Turkey. *Can. Mineral.* **40**, 895-908.

VERGNIOLLE, S., & MANGAN, M.(2001): Hawaiian and Strombolian eruptions. *In* Encyclopedia of Volcanoes (H. Sigurdsson, ed.). Academic Press, San Diego, California (447-461).

VON DAMM, K.L. (1995): Controls on the chemistry and temporal variability of sea floor hydrothermal fluids. *In* Sea Floor Hydrothermal Systems: Physical, Chemical, Biological, and Geological Interactions (S.E. Humphris, R.A. Zierenberg, L.S., Mullineaux & R.E. Thomson, eds.). *Am. Geophys. Union, Monogr.* **91**, 222-247.

WALLACE, P. & CARMICHAEL, I.S.E. (1992): Sulfur in basaltic magmas. *Geochim. Cosmochim. Acta* **56**, 1863-1874.

WHEAT, C.G., JANNASCH, H.W., PLANT, J.N., MOYER, C.L., SANSONE, F.J. & MCMURTRY, G.M. (2000): Continuous sampling of hydrothermal fluids from Loihi Seamount after the 1996 event. *J. Geophys. Res.* **105**, 19,353-19,367.

WHITE. M.W., HOFMAN, A.W. & PUCHELT, H. (1997): Isotope geochemistry of Pacific mid-ocean ridge basalt. *J. Geophys. Res.* **92**, 4881-4893.

WOODRUFF, L.G. & SHANKS, W.C., III (1988): Sulfur isotope study of chimney minerals and vent fluids from 21%N, East Pacific Rise: hydrothermal sulfur sources and disequilibrium sulfate reductions. *J. Geophys. Res.* **93**, 4562-4572.

ZIERENBERG, R.A., KOSKI, R.A., MORTON, J.L., BOUSE, R.M. & SHANKS, W.C., III (1993): Genesis of massive sulfide deposits on a sediment-covered spreading center, Escanaba Trough, southern Gorda Ridge. *Econ. Geol.* **88**, 2069-2098.

Received August 4, 2002, revised manuscript accepted January 30, 2003.